UDK 67.017:620.3:549.514.6
Original scientific article/Izvirni znanstveni članek

ISSN 1580-2949
MTAEC9, 55(1)19(2021)

MECHANICAL PROPERTIES OF ANODIC TITANIUM DIOXIDE NANOSTRUCTURES

MEHANSKE LASTNOSTI NANOSTRUKTUR TITANOVEGA DIOKSIDA

Mukta Kulkarni[1], Josef Šepitka[2], Ita Junkar[3], Metka Benčina[1,3], Niharika Rawat[1], Anca Mazare[4], Chandrashekhar Rode[5], Suresh Gokhale[6], Patrik Schmuki[4], Matej Daniel[2], Ales Iglič[1]*

[1]Laboratory of Physics, Faculty of Electrical Engineering, University of Ljubljana, Tržaška 25, 1000 Ljubljana, Slovenia
[2]Department of Mechanics, Biomechanics and Mechatronics, Faculty of Mechanical Engineering, Czech Technical University in Prague, Technicka 4, Prague 16607, Czech Republic
[3]Department of Surface Engineering and Optoelectronics, Jožef Stefan Institute, Jamova 39, 1000 Ljubljana, Slovenia
[4]Department of Materials Science and Engineering, WW4-LKO, University of Erlangen Nürnberg, Martensstrasse 7 91058, Erlangen, Germany
[5]Chemical Engineering and Process Development Division, CSIR-National Chemical Laboratory, Dr. Homi Bhabha Road, Pune, India 411008
[6]Physical & Materials Chemistry Division, CSIR-National Chemical Laboratory, Dr. Homi Bhabha Road, Pune, India 411008

Prejem rokopisa – received: 2020-06-09; sprejem za objavo – accepted for publication: 2020-07-25

doi:10.17222/mit.2020.109

Highly ordered and uniform titanium dioxide (TiO_2) nanotubes (NTs) with different morphologies (15 nm, 50 nm and 100 nm in diameter) were prepared by the electrochemical anodization of Ti substrates. The TiO_2 NTs' surface properties were characterized by X-ray diffraction (XRD) spectroscopy, Raman spectroscopy, scanning electron microscopy (SEM) and atomic force microscopy (AFM). The elastic modulus (E) and the Vickers hardness (HV) of the Ti foil and of the different-morphology TiO_2 NTs were evaluated with the nano-indentation technique. E and HV increase with the decreasing length/diameter of the NTs, meaning that NTs with smaller diameters are more resistant to mechanical wear. The elastic modulus of the TiO_2 NTs with 15-nm and 50-nm diameters is similar to that of the human bone.

Keywords: titanium dioxide (TiO_2) nanotubes, mechanical properties, elastic modulus, Vickers hardness

Z elektrokemično anodizacijo titanovega (Ti) substrata smo pripravili nanocevke iz titanovega dioksida (TiO_2) z različno morfologijo. Pripravljene TiO_2 nanocevke smo karakterizirali z rentgensko difrakcijsko spektroskopijo (XRD), Ramansko spektroskopijo, vrstično elektronsko mikroskopijo (SEM) in mikroskopijo na atomsko silo (AFM). Elastični modul (E) in Vickersova trdota (HV) Ti folije in TiO_2 nanocevk z različno morfologijo, sta bili določeni s tehniko nanoindentacije. Elastični modul in Vickersova trdota naraščata z zmanjšanjem dolžine/premera TiO_2 nanocevk, kar pomeni, da so nanocevke z nižjim premerom bolj odporne na mehansko obrabo. Elastični modul TiO_2 nanocevk, s premerom 15 nm in 50 nm, je podoben elastičnemu modulu človeških kosti.

Ključne besede: nanocevke iz titanovega dioksida (TiO_2), mehanske lastnosti, elastični modul, Vickersova trdota

1 INTRODUCTION

Titanium and its alloys are some of the most widely used implant materials because of their low toxicity, biocompatibility and mechanical properties. This is attributed to great tensile strength, resistance to body fluid effects, flexibility and high corrosion resistance.[1] Although orthopaedic implants made of titanium alloys imply better results, the limited lifetime of these implants remains a major drawback. This limitation is due to the integration of the Ti-implant material with the juxtaposed bone tissue (osseointegration).[2,3] To overcome osseointegration, the surface of titanium and its alloys can be modified to support cell adhesion and to encourage the formation of new bone at the interface between the implant surface and the bone tissue.[4]

Surface modification involves shifting topography from the micro to nanoscale or tailoring the nanoscale morphology so that the implant surface mimics the feature size of natural tissues and promotes cellular functions.[5,6] Fabricating implant surfaces to have nanoscale dimensions is important because the feature size of all tissues is in the nano regime. For example, natural bone has inorganic constituent made up of 2–5 nm thickness and 20–25 nm wide hydroxyapatite crystals.[7] Electrochemical anodization is one of the most cost-effective and convenient methods of nanoscaling the surface,[8–10] which when performed under self-organized conditions results in TiO_2 NTs grown directly on the Ti substrate material.[1–9] In addition, the morphology of the nanotubes can be tailored for the desired application, e.g., the thickness of these layers can reach several hundreds of μm, while the nanotube diameter can be adjusted from 10 nm to 800 nm.[1,11] Among all the other properties of TiO_2 nanostructures, the elastic modulus is a property that affects directly the implant stability. It is desirable that the

*Corresponding author's e-mail:
ales.iglic@fe.uni-lj.si (Aleš Iglič)

metal's elastic modulus be as close as possible to that of the bone, because smaller differences between these values will result in a better transfer of stress, and avoiding the stress-shielding effect.[12]

The elastic modulus and hardness of the TiO_2 NTs layer plays an important role for the long-term stability of the implant – the most suitable technique to determine the elastic modulus of such thin TiO_2 oxide layers is nano-indentation. However, the initial roughness and the probe geometry impose limitations. G. A. Crawford et al.[13] have examined the deformation behaviour of a nanotube layer using nano-indentation tests with a Berkovich probe, that led to an indentation penetration higher than the thickness of the nanotube layer and wear marks on the indentation. B. Voltrova et al.[14] studied the influence of the TiO_2 nanotubes' diameter on the nanomechanical properties and found that a larger diameter of the nanotubes showed a lower elastic modulus and indentation hardness, and indicated that TiO_2 nanotubes with a diameter close to 66 nm show the highest in-vitro benefits and therefore could be applied to improve bone implants' osseointegration.

In the present study, TiO_2 NTs with different morphologies were obtained by using electrochemical anodization and the nano-indentation properties of different diameter nanotubes were studied based on the Oliver-Pharzz methodology.

2 EXPERIMENTAL PART

2.1 Materials

Titanium foil (Advent Research Materials, 0.1 mm thickness, 99.6 %), ethylene glycol (Fluka, ≥99.5 %), ammonium fluoride – NH_4F (Sigma Aldrich, 28.0–30.0 %), hydrofluoric acid – HF (Sigma Aldrich, ≥40 %) acetone (Honeywell Riedel – de Haen, 99.5 %), ethanol (Sigma Aldrich, 96%), deionized water (miliQ).

2.2 Fabrication of TiO_2 nanosurfaces

The fabrication of the TiO_2 NTs was carried out according to the electrochemical anodization method as in references,[5–8] although using slightly different parameters, as described below. All the anodization experiments were carried out at room temperature (~20 °C) in a two-electrode system, using Ti foil as the working electrode and a platinum gauze as the counter electrode. Prior to anodization, the Ti foils were degreased by successive ultrasonication in acetone, ethanol and deionised water for 5 min each and dried in a nitrogen stream. An ethylene glycol-based electrolyte containing NH_4F (0.35 *w*/%) and H_2O (1.7 *w*/%) was used to grow the TiO_2 NTs. This step was followed by removing the nanotubular layer via ultrasonication in deionised water and then by drying the pre-patterned sample in a nitrogen stream. This pre-patterned surface was subsequently used as a substrate in the anodization in the ethylene-glycol-based electrolyte containing hydrofluoric acid (**Table 1**), used to grow homogeneous layers of self-arranged TiO_2 NTs. The as-formed TiO_2 NTs were immersed in ethanol for 2 h in order to remove the organic components from the electrolyte solution.

2.3 Surface characterization of Ti nanostructures

2.3.1 Scanning Electron Microscopy (SEM)

The morphology of the TiO_2 nanostructures was observed using a field-emission scanning electron microscope – Hitachi FE-SEM S4800.

2.3.2 Atomic Force Microscopy (AFM)

Topographic features of the Ti foil and of the 100-nm-diameter TiO_2 NTs were studied by Atomic Force Microscopy (Solver PRO, NT-MDT, Russia) in tapping mode in an air atmosphere. The samples were scanned with the standard Si cantilever (MikroMasch) at a constant force of 22 N/m and resonance frequency of 325 kHz (10 nm tip radius and 95 μm tip length). The average surface roughness (R_a) was calculated from 10 different images made on (5×5) μm areas.

2.3.3 Scanning Probe Microscopy (SPM)

The 3D topography of the titanium substrate surface was obtained by Hysitron's *in-situ* Scanning Probe Microscopy (SPM). Samples were scanned at a contact force of 1 μN between a nano-indentation tip (diamond Berkovich) and a titanium substrate surface. *In-situ* SPM images were analysed using Hysitron's TriboView™ software. The average surface roughness (R_a) was calculated from a (20×20) μm area. 3D topography of the TiO_2 NTs' surface was obtained by Hysitron's *in-situ* SPM as well. Samples were scanned at a contact force of 0.05 μN between the nano-indentation tip (diamond Cube Corner) and the TiO_2 NTs' surface.

2.3.4 Raman spectroscopy

Raman spectra of all TiO_2 samples were recorded using a Horiba Jobin-Yvon LabRAM HR800 Raman spectrometer equipped with 100× optical microscope, appropriate holographic notch filters and 1800 grooves/mm holographic grating to provide the spectral resolution of 0.25 cm^{-1}. A 632.8 nm helium-neon laser of 10-mW power and 2-μm spot size was used to excite the samples. The spectra were taken in the wavenumber range of 100–1000 cm^{-1} with an exposure time of 2s.

2.3.5 X-ray diffraction analysis (XRD)

The crystal structure of the nanotube arrays was also confirmed using X-ray diffraction (XRD; PAN analytical D8 model) with Cu-K_α radiation (K_α = 0,15400 nm) in the 2θ range 20–80.

2.3.6 Nanoindentation studies

A Hysitron TI 950 TriboIndenter™ nanomechanical test instrument was used for an assessment of the depth

Table 1: Influence of the anodization conditions used on the morphology (diameter and length) of TiO_2 NTs

Diameter (nm)	Electrolyte	Potential (V)	Anodization time (h)	Length (μm)
15	EG+8M H_2O+0.2M HF	10	2.5	0.22
50	EG+8M H_2O+0.2M HF	20	2.5	1.10
100	EG+8M H_2O+0.2M HF	58	2.5	3.50

profiles of the mechanical properties on TiO_2 NTs (diameters 15 nm, 50 nm and 100 nm) and Ti foil as a reference sample. The partial unload approach requires elastic-plastic deformation during gradual force cycles in order to analyse each unloading segment according the Oliver & Pharr method[15] Automated analysis plots the depth profile as discrete datasets. Based on the 1/10 rule, a coating of 100-nm thickness requires measurements at <10 nm depth.[16] A standard Berkovich tip area function $A(h)$, describing the shape of the indentation probe, was used: $A = 24.5h2 + C1h + C2h1/2 + C3h1/4 + C4h1/8 + C5h1/16$, where $C1 = 7.6736E+3$, $C2 = –2.3046E+5$, $C3 = 1.9088E+6$, $C4 = –4.2845E+6$ and $C5 = 2.6127E+6$. A Ti foil was used as reference to examine the nanomechanical properties of TiO_2 NTs with diameters of 15 nm, 50 nm and 100 nm.

Table 2: Number of TiO_2 NTs in the contact with the Berkovich tip for contact depth hc = 5 nm and hc = 35 nm corresponding to the diagram in **Figure 1** calculated from tip area function

Diameter (nm)	TiO_2 NTs in the contact hc = 5 nm (quantity)	TiO_2 NTs in the contact hc = 35 nm (quantity)
15	39.44	224.56
50	3.55	20.21
100	0.89	5.05

3 RESULTS

3.1 Morphology of TiO_2 NTs

The morphology of the TiO_2 NTs was evaluated with SEM. Analyses indicate the different diameters of the TiO_2 NTs (**Figure 2**), i.e., 15 nm, 50 nm and 100 nm with standard deviations of 20 %, 10 % and 5 %, respectively, that were achieved by changing the anodization potential used in the electrochemical anodization (**Table 1**).

The topographical features of the Ti foil used as a substrate for the growth of NTs, as well as of the TiO_2 NTs with 100 nm diameter were investigated by AFM,

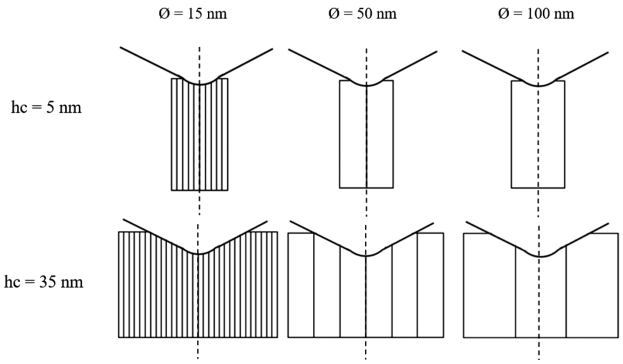

Figure 1: Schematic representation of contacts of the Berkovich indenter and TiO_2 NTs in the nano-indentation test

as presented in **Figure 3**. The AFM analysis of Ti foil shows that the surface is not fully uniform, and some vertical distortions (vertical roughness) are observed with the AFM (**Figure 3a**). The average surface roughness measured on a (5×5) μm area was about 35 nm. On the surface of the 100-nm-diameter TiO_2 NTs, features were clearly observed with the AFM, as the size of the nanotube diameter was sufficiently wide to enable the tip penetration inside the hollow nanotube interior, which was not possible for TiO_2 NTs with a smaller diameter, such as the TiO_2 NTs with 15 nm in diameter and TiO_2 NTs with a 50 nm in diameter. The average roughness measured on a (5×5) μm area for TiO_2 NTs with 100 nm in diameter was about 47 nm. However, it should be noted that this value is not entirely representative, as the AFM tip could only enter up to a limited length of the nanotube (as previously shown (8), the length of the TiO_2 NTs with 100 nm in diameter is about 3.5 μm as evaluated from SEM analysis). More importantly, the AFM results clearly show the opened hollow structure of the TiO_2 NTs as well as the slight deviations in their height, about 200 nm, as observed from the 3D image (**Figure 3b**).

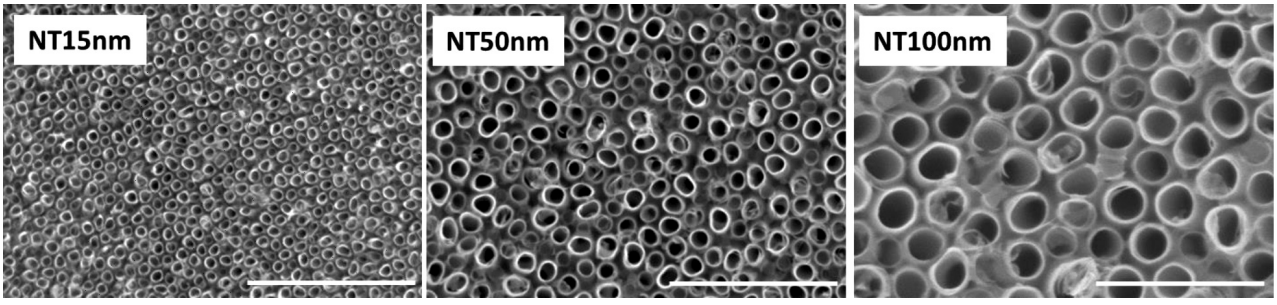

Figure 2: SEM images of the top surface of TiO_2 NTs (size of the scale bar=500 nm)

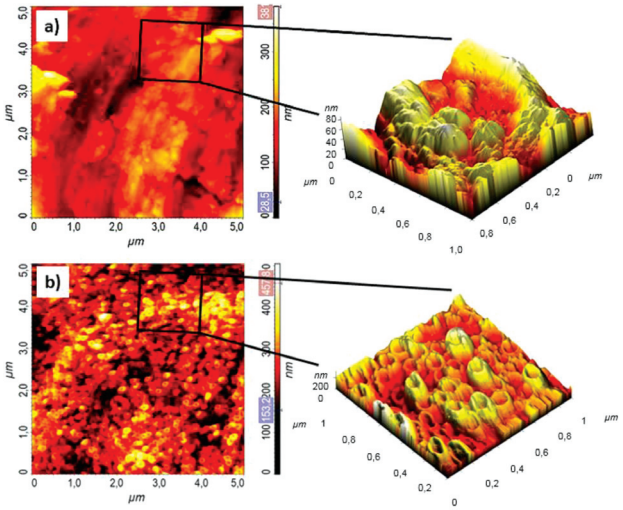

Figure 3: AFM images of: a) Ti foil, b) TiO_2 NTs with 100 nm in diameter. Zoomed region (along vertical *z*-direction) shows further topological details

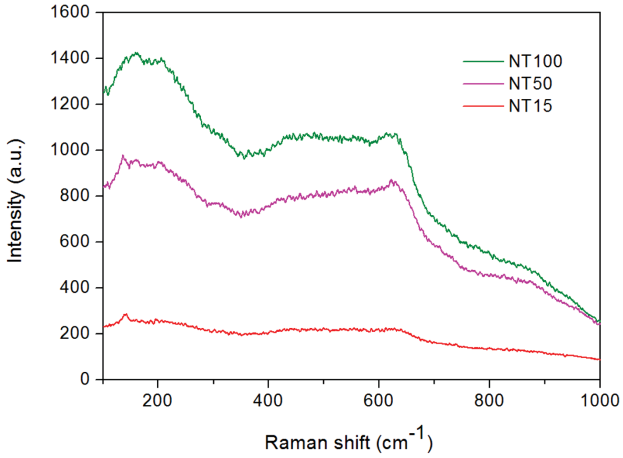

Figure 5: Raman spectra of TiO_2 NTs with various diameters. T=Ti substrate

The 3D topography of the titanium substrate (Ti foil) surface is also obtained by *in-situ* SPM, see **Figure 4a** and shows a non-negligible roughness of the sample. The average roughness of the Ti substrate surface was around 49 nm. Similarly, **Figures 4b** and **4c** show the *in-situ* SPM images of 100-nm-diameter TiO_2 nanotubes surface.

3.1.1 Crystal structure of TiO_2 NTs

Raman spectroscopy provides very important information about the Raman-active vibrational modes related to the Ti-Ti, Ti-O and O-O bonds in TiO_2. It is well known that anatase TiO_2 gives a strong Raman signal at 144 cm^{-1} followed by low intensity peaks at (197, 394-399, 513/514, 519 and 635-641) cm^{-1}, whereas rutile TiO_2 gives Raman signals at 143, 236/242, 446/447 and 610/613 cm^{-1}.[17–19] The Raman spectra for all TiO_2 samples of different diameters are presented in **Figure 5**. All the spectra show broad bands and no clear spectral characteristics of anatase or the rutile phase of TiO_2. Thus, the TiO_2 nanotubes produced in our electrochemical anodization process are of an amorphous nature [20] The broad bands appearing near 284 cm^{-1} and in the range 430–630 cm^{-1} in all the spectra can be assigned to O–O interactions consistent with the TiO_6^{8-} octahedral structure and the Ti-O interactions, respectively.(19) A sharp peak appearing at 143/144 cm^{-1} in the spectrum of the TiO_2 NTs with 15-nm diameter can be considered to arise from slightly rutile/anatase phase of TiO_2 nanotubes due to Ti–Ti covalent interactions. This feature tends to cease, and the amorphous nature tends to be more prominent as the tube diameter increases to 50 nm and 100 nm. The weak band near 840 cm^{-1} can be assigned as the first overtone of the 143/144 cm^{-1} band.[21]

The XRD patterns for the different diameter as-grown TiO_2 NT arrays as well as for the substrate material (Ti foil) are presented in **Figure 6**. After the electrochemical anodization, no crystalline phase is detected for the as-grown NTs, thus further confirming their amorphous state. Comparing the patterns of the TiO_2 NTs with that of the substrate materials only peaks characteristic for the Ti substrate materials are detected. These results are in agreement with the previous report.[22]

3.1.2 Nanoindentation studies

The mechanical stability of the implant is an essential factor to maintain its long-term success. In the present study, the mechanical properties of TiO_2 NTs with differ-

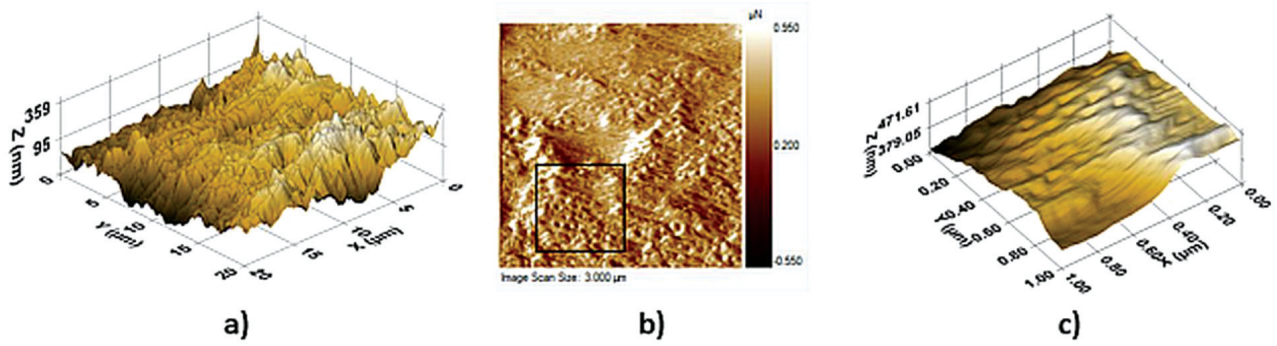

Figure 4: *In-situ* SPM images: a) 3D topography of titanium foil, b) map of gradients of forces obtained from TiO_2 NTs with 100 nm in diameter sample and c) 3D topography of the area demarcated by a black square in the picture from b)

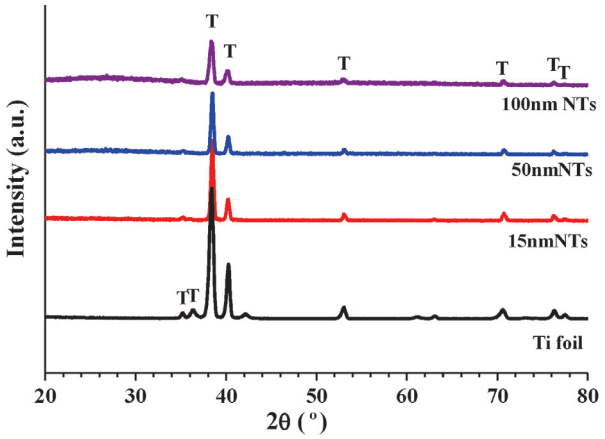

Figure 6: X-ray diffraction (XRD) patterns of Ti substrate and TiO_2 NTs with various diameters (T=Ti substrate)

ent lengths and diameters (**Table 1**) were measured with a Berkovich indenter. Values of *E* and HV (calculated from apparent indentation hardness *HIT*) were calibrated from contact depths *hc* = 5 nm and *hc* = 35 nm, respectively (**Figure 7**).[16]

In this work, the elastic modulus increases with decreasing diameter of the TiO_2 NTs, and with decreasing length as well. The evaluated *E* is 8.7±4.2 GPa for TiO_2 NTs with 100 nm in diameter, 10.3±4.6 GPa for TiO_2 NTs with 50 nm in diameter and 19.2±4.3 GPa for TiO_2 NTs with 15 nm in diameter (**Figure 8**). Y.N. Xu et al. [23] reported an elastic modulus of 5.1 GPa for longer TiO_2 NTs (~8.5 μm), with a diameter of ~199 nm and a wall thickness of ~14.3 nm. However, the elastic modulus of the 15-nm- and 50-nm-diameter TiO_2 NTs evaluated in the present study is similar to that of bone, which is 11–30 GPa.[24]

It has been reported that the hardness of films is dependent on their adhesion to the substrate, i.e., the higher the hardness, the higher the adhesion.[25] In present study, *Hv* increases with decreasing length/diameter of the NTs; therefore, TiO_2 NTs of 15 nm in diameter exhibit the highest adhesion strength to the substrate (**Figure 9**). Since adhesion is higher for smaller diameter TiO_2 NTs,

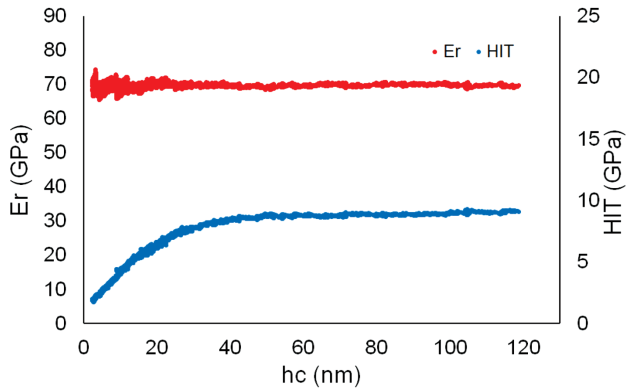

Figure 7: Calibration values of *E* and *H* vs. contact depth on fused quartz sample

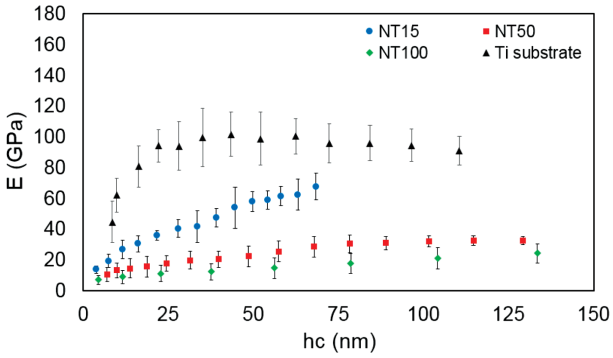

Figure 8: Depth profile of Young's modulus

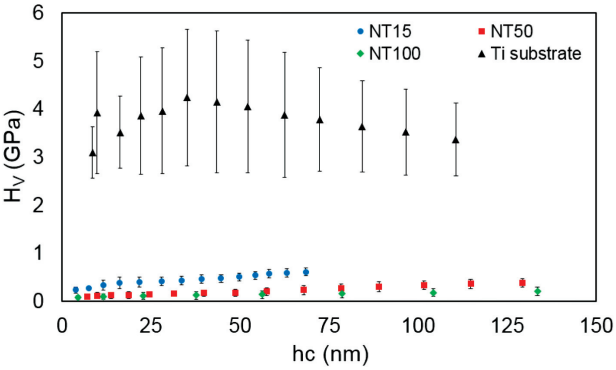

Figure 9: Depth profiles of calculated Vickers hardness. The Vickers hardness was calculated from the measured apparent indentation hardness *HV* (GPa) = 0.92666*HIT

it follows that such nanostructures are also more resistant to mechanical wear.[26] However, the *Hv* values are consistent with the existing reported values. For instance, Y. N. Xu et al.[23] reported a hardness of 0.094 GPa for longer TiO_2 NTs (diameter: approx. 199 nm, wall thickness: 1 approx. 14.3 nm and length: approx. 8.5 μm). In the present study, *Hv* is 0.45±0.09 GPa for TiO_2 NTs with 15 nm in diameter, 0.16±0.06 GPa for TiO_2 NTs with 50 nm in diameter and 0.12±0.08 GPa for TiO_2 NTs with 100 nm in diameter. The average *Hv* of the Ti foil is 3.8 ±0.3 GPa.

4 CONCLUSIONS

Amorphous, as-formed TiO_2 NTs with diameters of 15 nm, 50 nm and 100 nm were prepared by electrochemical anodization. The nano-indentation studies revealed that the elastic modulus and Vickers hardness of the TiO_2 NTs increased with the decreasing length/diameter of the TiO_2 NTs (as a reference, a Ti foil was measured). The elastic modulus of 15 nm and 50 nm diameter TiO_2 nanotubes is similar to the elastic modulus of the human bone. The Vickers hardness of the 15-nm-diameter TiO_2 nanotubes exhibits the highest adhesion strength to the substrate. These results indicate that the TiO_2 NTs with smaller diameters are more resistant to mechanical wear. Such materials can be used in medical

applications, such as orthopaedic implants or drug-delivery systems.

Acknowledgment

The authors would like to acknowledge the Slovenian Research Agency for financial support, grants No. Z3-4261 and J3-9262 and Slovenian Ministry of Education, Science and Sport grant "Public call for encouraging young investigators at the beginning of their career 2.0", No. 5442-15/2016/18.

5 REFERENCES

[1] P. Roy, S. Berger, P. Schmuki, TiO_2 Nanotubes: Synthesis and Applications, Angew. Chem. Int. Ed., 50 (**2011**) 13, 2904–2939, doi:0.1002/anie.201001374

[2] V. Sansone, D. Pagani, M. Melato, The effects on bone cells of metal ions released from orthopaedic implants, Clin. Cases Miner. Bone Metab., 10 (**2013**) 1, 34–40, doi:10.11138/ccmbm/2013.10.1.034

[3] M. Izmir, B. Ercan, Anodization of titanium alloys for orthopedic applications, Front. Chem. Sci. Eng., 13 (**2019**) 1, 28–45, doi:10.1007/s11705-018-1759-y

[4] E. P. Su, D. F. Justin, C. R. Pratt, V. K. Sarin, V. S. Nguyen, S. Oh, & S. Jin, Effects of titanium nanotubes on the osseointegration, cell differentiation, mineralisation and antibacterial properties of orthopaedic implant surfaces, The Bone & joint J., 100 (**2018**), 9–16, doi:10.1302/0301-620X.100B1.BJJ-2017-0551.R1

[5] M. Kulkarni, A. Flašker, M. Lokar, K. Mrak-Poljšak, A. Mazare, A. Artenjak, S. Čučnik, S. Kralj, A. Velikonja, P. Schmuki, Binding of plasma proteins to titanium dioxide nanotubes with different diameters, Int. J. Nanomed., 10 (**2015**) 1, 1359–1373, doi:10.2147/IJN.S77492

[6] K. S. Brammer, S. Oh, C. J. Cobb, L. M. Bjursten, H. V. D. Heyde, S. Jin, Acta Biomater., 5 (**2009**) 8, 3215–3223, doi:10.1016/j.actbio.2009.05.008

[7] L. C. Palmer, C. J. Newcomb, S. R. Kaltz, E. D. Spoerke, S. I. Stupp, Biomimetic systems for hydroxyapatite mineralization inspired by bone and enamel, Chem. Rev., 108 (**2008**) 11, 4754–4783, doi:10.1021/cr8004422

[8] M. Kulkarni, Y. Patil-Sen, I. Junkar, C. V. Kulkarni, M. Lorenzetti, A. Iglič, Wettability studies of topologically distinct titanium surfaces, Coll. and Surf. B: Biointerfaces, 129 (**2015**), 47–53, doi:10.1016/j.colsurfb.2015.03.024

[9] M. Kulkarni, A. Mazare, E. Gongadze, Š. Perutkova, V. Kralj-Iglič, I. Milošev, P. Schmuki, A. Iglič, M. Mozetič, Titanium nanostructures for biomedical applications, Nanotechnology, 26 (**2015**) 6, 062002, doi:10.1088/0957-4484/26/6/062002

[10] D. Kowalski, D. Kim, P. Schmuki, TiO_2 nanotubes, nanochannels and mesosponge: Self-organized formation and applications, Nano today, 8 (**2013**) 3, 235–264, doi:10.1016/j.nantod.2013.04.010

[11] K. Lee, A. Mazare, P. Schmuki, One-Dimensional Titanium Dioxide Nanomaterials: Nanotubes, Chemical reviews, 114 (**2014**) 19, 9385–9454, doi:10.1021/cr500061m

[12] M. Niinomi, M. Nakai, Titanium-Based Biomaterials for Preventing Stress Shielding between Implant Devices and Bone, Int. J. Biomaterials, 2011 (**2011**), doi:10.1155/2011/836587

[13] G. A. Crawford, N. Chawla, K. Das, S. Bose, A. Bandyopadhyay, Microstructure and deformation behavior of biocompatible TiO_2 nanotubes on titanium substrate, Acta Biomater., 3 (**2007**) 3, 359–367, doi:10.1016/j.actbio.2006.08.004

[14] B. Voltrova, V. Hybasek, V. Blahnova, J. Sepitka, V. Lukasova, K. Vocetkova, V. Sovkova, R. Matejka, J. Fojt, L. Joska, M. Daniel, E. Filova, Different diameters of titanium dioxide nanotubes modulate Saos-2 osteoblast-like cell adhesion and osteogenic differentiation and nanomechanical properties of the surface, RSC Advances, 9 (**2019**) 20, 11341–11355, doi:10.1039/c9ra00761j

[15] G. Pharr, W. Oliver, Measurement of Thin Film Mechanical Properties Using Nanoindentation, MRS Bulletin, 17 (**1992**) 7, 28–33, doi:10.1557/S0883769400041634

[16] B. STANDARD, B. ISO, Metallic materials – Instrumented indentation test for hardness and materials parameters, (**2007**)

[17] V. Castrejón-Sánchez, E. Camps, M. Camacho-López, Quantification of phase content in TiO_2 thin films by Raman spectroscopy, Superficies y vacío, 27 (**2014**) 3, 88–92

[18] F. Tian, Y. Zhang, J. Zhang, C. Pan, Raman spectroscopy: a new approach to measure the percentage of anatase TiO_2 exposed (001) facets, J. Phys. Chem. C, 116 (**2012**) 3, 7515–7519, doi:10.1021/jp301256h

[19] F. D. Hardcastle, Raman spectroscopy of titania (TiO_2) nanotubular water-splitting catalysts. Journal of the Arkansas academy of science, 65 (**2011**) 1, 43–48

[20] H. Yin, Y. Wada, T. Kitamura, S. Kambe, S. Murasawa, H. Mori, T. Sakata, S. Yanagida, Hydrothermal synthesis of nanosized anatase and rutile TiO_2 using amorphous phase TiO_2, J. Mater. Chem., 11 (**2001**) 6, 1694–1703, doi:10.1039/b008974p

[21] U. Balachandran, N. G. Eror, Raman spectra of titanium dioxide. Journal of Solid State Chemistry, 42 (**1982**) 3, 276–282, doi:10.1016/0022-4596(82)90006-8

[22] G. K. Mor, O. K. Varghese, M. Paulose, K. Shankar, C. A. Grimes, A review on highly ordered, vertically oriented TiO_2 nanotube arrays: Fabrication, material properties, and solar energy applications. Solar Energy Materials and Solar Cells, 90 (**2006**) 14, 2011–2075, doi:10.1016/j.solmat.2006.04.007

[23] Y. N. Xu, M. N. Liu, M. C. Wang, A. Oloyede, J. M. Bell, C. Yan, Nanoindentation study of the mechanical behavior of TiO_2 nanotube array, Journal of Applied Physics, 118 (**2015**) 14, 145301, doi:10.1063/1.4932213

[24] J. Y. Rho, T. Y. Tsui, G. M. Pharr, Elastic properties of human cortical and trabecular lamellar bone measured by nanoindentation, Biomaterials, 18 (**1997**) 20, 1325–1330, doi:10.1016/S0142-9612(97)00073-2

[25] D. Stone, W. R. LaFontaine, P. Alexopoulos, T. W. Wu, C. Y. Li, An investigation of hardness and adhesion of sputter-deposited aluminum on silicon by utilizing a continuous indentation test, J. Materials Research, 3 (**1988**) 1, 141–147, doi:10.1557/JMR.1988.0141

[26] S. A. Alves, A. L. Rossi, A. R. Ribeiro, F. Toptan, A. M. Pinto, T. Shokuhfar, J.-P. Celis, L. A. Rocha, Improved tribocorrosion performance of bio-functionalized TiO_2 nanotubes under two-cycle sliding actions in artificial saliva, Journal of the mechanical behavior of biomedical materials, 80 (**2018**), 143–154, doi:10.1016/j.jmbbm.2018.01.038